Pamukkale Üniversitesi Mühendislik Bilimleri Dergisi
Pamukkale University Journal of Engineering Sciences

Performance comparison of boost and super-lift Luo converters in solar energy systems using fuzzy logic-based MPPT control

Bulanık mantık tabanlı MPPT kontrolü kullanan güneş enerjisi sistemlerinde yükselten ve süper-lift Luo dönüştürücülerin performans karşılaştırması

Murat Tören[1], Bengisu Kaba[1], Gokturk Ozturk[2]*

[1]Department of Electrical And Electronics Engineering, Recep Tayyip Erdoğan University, Rize, Türkiye.
murat.toren@erdogan.edu.tr, bengisu_kaba23@erdogan.edu.tr
[2]Department of Energy Systems Engineering, Recep Tayyip Erdoğan University, Rize, Türkiye.
gokturk.ozturk@erdogan.edu.tr

Received/Geliş Tarihi: 13.08.2025 Revision/Düzeltme Tarihi: 22.10.2025 doi: 10.65206/pajes.92724
Accepted/Kabul Tarihi: 03.11.2025 Research Article/Araştırma Makalesi

Abstract

This study implements a fuzzy logic-based control mechanism integrated with a super-lift Luo converter to achieve maximum power point tracking (MPPT) in solar energy systems. A comparative analysis of two distinct converter topologies, Boost and Super-lift Luo - an approach not commonly found in similar studies - and constitutes an original component of our research, has been conducted in the context of a DC-DC converter block within the control system. A fuzzy logic controller has been developed as the MPPT algorithm for both systems, utilizing identical solar panel conditions. The super-lift Luo converter has roughly 4% greater efficiency than the conventional boost converter, offering enhanced voltage gain and reduced input current. Furthermore, it has been established that the system utilizing the super-lift Luo converter is better suited for high-power loads and industrial applications. The stability of both systems was verified under sudden changes in environmental parameters, demonstrating their ability to maintain the maximum power point without oscillations or instability. The engineered controller configuration has enabled both converters to achieve steady output values and function at the maximum power point without overshooting. Moreover, additional research was conducted under diverse irradiance and temperature conditions and at varied load levels, to assess system robustness and dynamic response. These investigations also highlighted the suitability of fuzzy logic control for real-time embedded PV applications, due to its low computational burden and strong adaptability to nonlinear behaviours. The results obtained distinctly demonstrate the influence of converter type and control methodology on system performance.

Keywords: Fuzzy logic, Super-lift Luo, Solar energy systems, MPPT

Öz

Bu çalışmada, güneş enerjisi sistemlerinde maksimum güç noktası takibi (MPPT) elde etmek için süper-lift Luo dönüştürücü ile entegre edilmiş bulanık mantık tabanlı bir kontrol mekanizması uygulanmaktadır. Benzer çalışmalarda yaygın olarak bulunmayan bir yaklaşım olan ve araştırmamızın orijinal bir bileşenini oluşturan iki farklı dönüştürücü topolojisi olan Yükselten ve Süper-lift Luo'nun karşılaştırmalı bir analizi, kontrol sistemi içindeki bir DC-DC dönüştürücü bloğu bağlamında gerçekleştirilmiştir. Her iki sistem için MPPT algoritması olarak, aynı güneş paneli koşullarını kullanan bir bulanık mantık denetleyicisi geliştirilmiştir. Çalışmada süper-lift Luo dönüştürücü, geleneksel yükselten dönüştürücüye göre yaklaşık %4 daha fazla verimliliğe sahiptir ve gelişmiş voltaj kazancı ve azaltılmış giriş akımı sunmaktadır. Ayrıca, süper-lift Luo dönüştürücü kullanan sistemin yüksek güçlü yükler ve endüstriyel uygulamalar için daha uygun olduğu tespit edilmiştir. Her iki sistemin kararlılığı, çevresel parametrelerdeki ani değişiklikler altında doğrulanmış ve salınım veya kararsızlık olmadan maksimum güç noktasını koruma yeteneklerini göstermiştir. Tasarlanan kontrolör konfigürasyonu, her iki dönüştürücünün de sabit çıkış değerleri elde etmesini ve aşım olmadan maksimum güç noktasında çalışmasını sağlamıştır. Ayrıca, sistemin sağlamlığını ve dinamik tepkisini değerlendirmek için farklı ışınım ve sıcaklık koşulları altında ve çeşitli yük seviyelerinde ek araştırmalar yapılmıştır. Bu araştırmalar aynı zamanda bulanık mantık kontrolcünün uygunluğunu da vurgulamıştır.

Anahtar kelimeler: Bulanık mantık, Süper-lift Luo, Güneş enerji sistemleri, MPPT

1 Introduction

A variety of algorithms have been employed to enhance energy efficiency and improve maximum power point tracking (MPPT) in renewable energy systems. In recent years, fuzzy logic controllers (FLC) have exhibited enhanced control effectiveness relative to conventional approaches. The implementation of FLC-based control in a hybrid renewable energy system resulted in a 30% reduction in fuel consumption and a 15% enhancement in system efficiency [1]. A study combining Perturb and Observe (P&O) with FLC revealed that the FLC-MPPT algorithm exhibited reduced power fluctuation and greater resilience to fluctuating weather conditions than standard P&O [2]. Experimental findings highlight the performance differences between the FLC-based P&O algorithm and the conventional P&O approach. The research indicates that the FLC-based P&O algorithm outperforms the traditional P&O algorithm [3]. A comparative evaluation of the FLC-P&O structure and flexible P&O algorithms revealed that the FLC-P&O structure resulted in reduced power fluctuations and shown enhanced performance regarding oscillation, response time, and computational accuracy [4]. In a similar manner, to harness the advantageous impacts of FLC within the system, FLC will be implemented in both systems developed in

*Corresponding author/Yazışılan Yazar

the study. Instead of comparing the controllers, the impact of FLC on two distinct types of converters inside a solar energy system will be analyzed.

Various control methods for MPPT in photovoltaic (PV) systems, together with their comparisons to FLC, are documented in the literature. A study comparing FLC with the incremental conductance (InC) algorithm revealed that FLC attained the maximum power point more rapidly than InC, exhibited reduced fluctuation, and demonstrated superior efficiency [5]. In a study comparing InC with FLC, a commercial photovoltaic system was examined utilizing the dSPACE platform. The study concluded that FLC demonstrated superior performance compared to InC regarding steady-state oscillation, response time, and overshoot [6]. A comparative evaluation of the FLC and InC algorithms revealed that FLC more efficiently mitigated voltage variations than InC. Simultaneously, FLC has exhibited a more rapid and effective response to fluctuating weather conditions than InC. Consequently, FLC has been employed instead of InC for enhanced system stability and efficiency. [7]. A comparative examination of the P&O, InC, and FLC algorithms highlights the advantages of the FLC approach. The results show that FLC delivers more consistent output power under fluctuating irradiation and transient faults. Furthermore, the study confirms that FLC achieves higher efficiency compared to the InC and P&O algorithms [8]. A study highlighted the rapid responsiveness of FLC to environmental changes and its insensitivity to circuit parameter variations, in contrast to InC and P&O, in a PV-powered battery system [9]. In a separate investigation comparing particle swarm optimization (PSO), FLC, and P&O algorithms revealed that FLC and PSO exhibited superior efficiency relative to the P&O approach. The study attained an efficiency value of 97.38% using FLC [10]. In assessing the superiority of FLC compared to alternative control techniques, this study will utilize FLC for the regulation of converters to guarantee optimal system efficiency. The study will also analyze the modifications necessary for the FLC algorithm in the PV systems developed using the boost and super-lift Luo converter topologies.

In contrast to traditional MPPT methods that rely on specific parameter tuning or mathematical modeling (such as P&O or InC), FLC provides adaptable rule-based control and can maintain accurate MPPT performance under dynamic and partially shaded conditions. Numerous comparison studies have repeatedly shown that FLC surpasses conventional approaches in terms of tracking speed, reduced oscillations, and overall efficiency [11, 12]. Considering system requirements and environmental factors, FLC stands out as one of the most efficient MPPT systems based on our simulation results and recent findings in literature.

On the other hand, Artificial Neural Networks (ANN) may demonstrate superior theoretical efficiency owing to their learning capabilities; however, they frequently require substantial computational resources, resulting in delays and constraining their applicability in real-time scenarios. Conversely, FLC provides a harmonious blend of robustness, efficiency, and simplicity, rendering it more suitable for embedded PV systems requiring rapid and dependable responses [13].

Figure (1) illustrates a column graph comparing the efficiency of various control methods (FLC, InC, P&O, ANN).

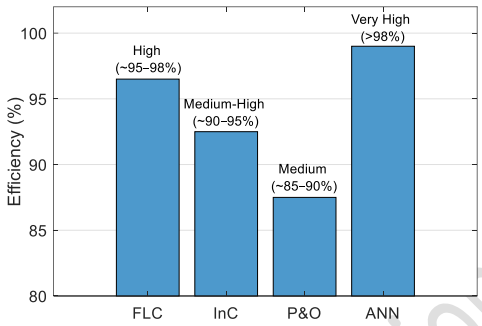

Figure 1. Efficiency comparison of several control systems.

A comparative evaluation of FLC against commonly utilized MPPT methodologies is offered to endorse the adoption of FLC as the control strategy for converter control. FLC is acknowledged for its efficacy in managing nonlinear systems with uncertainties, independent of exact mathematical description. Table 1 juxtaposes the FLC method with InC, P&O, and ANN, emphasizing performance criteria including decision correctness and adaptability.

Table 1. Comparative analysis of MPPT control algorithms.

Control Algorithm	Decision Accuracy	Adaptability
FLC	High. Able to make human-like decisions in uncertain conditions.	Medium-High. Effortlessly modified using rule-based logic.
InC	Medium. Responsive to variations in voltage and current.	Low. Predicated on fixed logic.
P&O	Low-Medium. Influenced by fluctuations, solely takes into account the direction of variation.	Low. Inability to proficiently adjust to system dynamics.
ANN	High. Elevated precision contingent upon training data.	High. Can swiftly acclimate to novel circumstances by learning.

Research is also being undertaken on converters utilized in renewable energy systems, alongside control systems. The research in power electronics underscore the significance of converters in renewable energy systems. A research on hydroelectric systems compared the classical boost converter with the Luo converter. The traditional boost converter exhibited a system efficiency of 75%, whereas the super-lift Luo converter attained an efficiency of 98%. Simultaneously, the settling and rising durations have been decreased while employing the super-lift Luo [14]. A study showed that a hybrid renewable energy system, integrating solar and wind energy, was stabilized with a PI controller, resulting in the super-lift Luo converter achieving an efficiency of 96%. The research highlighted that the super-lift Luo converter provides a sustainable and economical alternative for renewable energy systems [15]. In the hybrid renewable energy system utilizing wind and solar energy, the super-lift Luo converter was employed alongside the P&O algorithm. The study proposed utilizing the super-lift Luo converter for hybrid power generation and optimizing the system size if additional resources were required [16]. While most of the studies discussed previously have focused on hybrid energy systems, the present work investigates the performance of classical

Boost and super-lift Luo converters controlled by fuzzy logic in a solar energy system. The objective is to enhance efficiency using the converter and the FLC algorithm. A study demonstrated that a hybrid renewable energy system, governed by a grey wolf optimization (GWO)-based MPPT algorithm, utilized the Luo converter to stabilize voltage and mitigate energy fluctuations [17]. A study comparing the P&O and FLC algorithms for MPPT in solar energy systems also employed a super-lift Luo converter. In the MATLAB/Simulink environment and under varying levels of solar irradiance, the FLC algorithm demonstrated more precise and stable maximum power tracking than the P&O method, thereby enhancing system efficiency [18]. In another study utilizing the super-lift Luo converter, an interval type-2 fuzzy neural network (IT2FNN)-based controller was implemented. The controller demonstrated lower settling time, recovery time, and steady-state error compared to the interval type-2 fuzzy controller (IT2FC) and conventional PI controller. Simulations under varying reference voltages, input voltages, and load conditions confirmed the superior performance of the IT2FNN [19]. An interval type-2 Takagi-Sugeno-Kang fuzzy logic controller (IT2-TSK-FLC) was implemented for a super-lift Luo converter in a PV system. To enhance MPPT and control stability, it was optimized using the Firefly Algorithm (FA). Comparative simulations under challenging environmental conditions demonstrated that the optimized IT2-TSK-FLC-FA controller reduced settling time by over 56%, increased efficiency by up to 10%, and provided improved control signal stability compared to the standard IT2-TSK-FLC [20]. A study was conducted on a super-lift Luo converter, evaluating system performance through a P&O-based MPPT method. This converter demonstrates consistent current output across varying load conditions and adjusts to changes in irradiation and temperature [21]. Compared to this study, the present work also employs the same type of converter; however, converter control is performed using FLC instead of the traditional P&O algorithm. In a study utilizing super-lift Luo and optimizing the MPPT process through artificial neural network (ANN)-based control approaches, it was found that controllers with dynamic learning rates yielded more stable voltage and power output than static methods [22]. A study evaluating Cuk, Buck-Boost, SEPIC, Boost, Zeta, Ultra-Lift Luo, and Super-Lift Luo converters under partial shading conditions revealed that the super-lift Luo converter yielded the maximum output voltage and power. Luo-based converters enhance system durability by functioning at low duty cycles [23].

This study will analyze the system response resulting from the integrated usage of converters and control structures, anticipated to demonstrate superior performance compared to traditional control methods and converters in photovoltaic systems. The project aims to enhance system efficiency by employing the FLC algorithm, recognized for its efficacy in PV systems, in conjunction with the super-lift Luo converter. The distinction between the converter and traditional converters is concurrently being analyzed. This will elucidate the alterations in the FLC structure and optimize the system's operational efficiency.

2 Solar energy systems

Solar energy is the most plentiful renewable energy source globally. In solar energy systems, solar radiation is transformed into electrical energy by PV devices [24]. The photovoltaic cells are the initial recipients of solar radiation. Figure (2) illustrates the single diode model of the photovoltaic cell. Light photons are essential for the conduction of current in these photovoltaic cells. The current flowing through the PV cell is associated with the cell voltage as delineated by the Shockley Diode Equation. This link is illustrated in Equation 1. The instantaneous photo-voltaic current depicted in the circuit is ex-pressed by Equation (2).

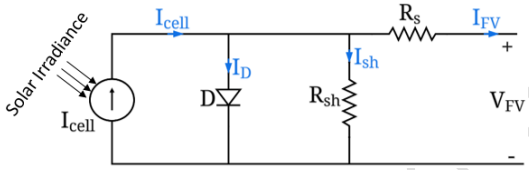

Figure 2. The single diode model of PV cell.

$$I_D = I_S\left(e^{(V_{FV}+I_{FV}R_s)/\eta V_T} - 1\right) \quad (1)$$

$$I_{FV} = I_{cell} - I_S\left(e^{(V_{FV}+I_{FV}R_s)/\eta V_T} - 1\right) - \frac{V_{FV}+I_{FV}R_s}{R_{sh}} \quad (2)$$

In this context, I_D, I_S and V_T represent the current through the diode, reverse saturation current and thermal voltage, respectively. η represents the ideality factor. The I_S value typically ranges from 10^{-6} to 10^{-5} A. η assumes a value within the range of 1 to 2. The calculation of thermal voltage is illustrated in Equation (3).

$$V_T = \frac{kT}{q} \quad (3)$$

T denotes the temperature measured in Kelvin. k represents the Boltzmann constant, valued at 1.381 x 10^{-23} J/K. q denotes the electron charge, valued at 1.602 x 10^{-19} C [25], [26].

In solar energy systems, uncontrollable external factors such as sun irradiation and temperature influence the current and voltage outputs of the photovoltaic (PV) panel. Consequently, the current-voltage and power-voltage graphs are likewise non-linear. These nonlinear graphs have a singular maximum power point (MPP) [27]. Figure (3) presents the current-voltage and power-voltage characteristics of a standard PV panel.

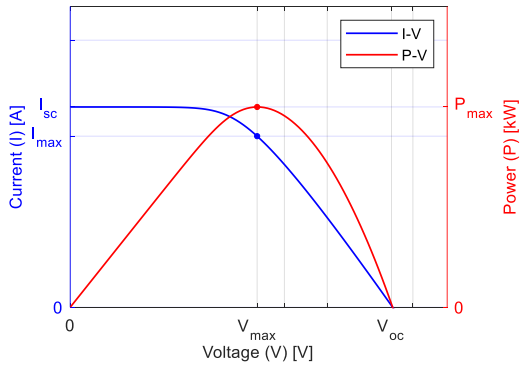

Figure 3. Current-voltage and power-voltage characteristics of a typical PV panel.

There are various ways for MPPT in solar energy systems. Current solar energy systems employ the P&O algorithm for MPPT. Nonetheless, prior research indicates that FLC has superior efficiency compared to P&O. Consequently, in this investigation, FLC was favored over P&O.

3 Converters

3.1 Boost converter

Primary circuit schematic the boost converter circuit illustrated in Figure (4) elevates the input voltage according to the signal sent to the switch component inside the circuit. The signal transmitted to the switch dictates its open or closed status. The circuit equations vary according to the switch's position [28], [29]. When the switch is closed, the circuit equations are represented by Equations (4 and 5); when the switch is open, the circuit equations are represented by Equations (6 and 7).

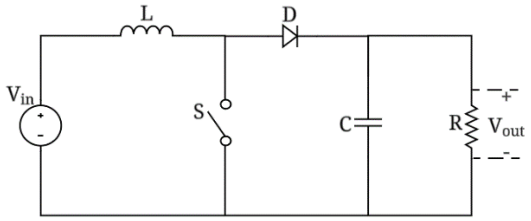

Figure 4. Circuit diagram of boost converter.

Switch on;

$$V_L = V_{in} = L\frac{di_L}{d_t} \tag{4}$$

$$(\Delta i_L)_{on} = \frac{V_{in}DT}{L} \tag{5}$$

Switch off;

$$V_L = V_{in} - V_{out} = L\frac{di_L}{d_t} \tag{6}$$

$$(\Delta i_L)_{off} = \frac{(V_{in} - V_{out})(1-D)T}{L} \tag{7}$$

In this context, V_{in} denotes the input voltage, V_L signifies the inductor voltage, and V_{out} indicates the output voltage, whilst i_L represents the current traversing the inductor. T represents the period, whereas D denotes the duty cycle.

3.2 Super-lift Luo converter

Super-lift Luo converters are engineered to deliver increased voltage amplification. In traditional converters, the output voltage rises arithmetically, however in the super-lift Luo converter, the output voltage is augmented geometrically [29]. Also, this converter design distinguishes itself from traditional boost converters by providing markedly better voltage gain and enhanced overall efficiency. It attains high output levels without necessitating excessive duty cycles or intricate multi-stage setups, rendering it a more pragmatic and efficient alternative. Furthermore, the super-lift Luo converter exhibits little output voltage and current ripple, rendering it a safer and more dependable choice for sensitive electrical applications where ripple mitigation is crucial. This study incorporates the super-lift Luo converter in a comparison examination with the commonly utilized boost converter topology in solar energy systems.

Figure (5) illustrates the primary circuit diagram of the converter. The converter has a single inductor (L), a switching element (S), a resistive load (R), two diodes (D_1, D_2), and two capacitors (C_1, C_2).

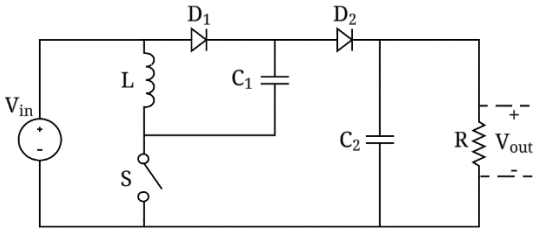

Figure 5. Circuit diagram of super-lift Luo converter.

The voltage gain of the super-lift Luo converter is determined using Equation (8).

$$G = \frac{V_{out}}{V_{in}} = \frac{2-k}{1-k} \tag{8}$$

In this context, G represents the voltage transfer gain, V_{out} denotes the output voltage, V_{in} signifies the input voltage, and k indicates the conversion ratio. The voltage gain equation stipulates that the conversion ratio must not exceed 1.

The converter circuit varies based on the switch position. Figure (6) illustrates the circuit schematics corresponding to the open and closed states of the switch. When the switch is closed, the D_1 diode conducts within the circuit. In this instance, energy is accumulated in the L and C_1 components as a result of the closed loops established at the input. When the switch is opened, only the D_2 diode conducts within the circuit. The L and C_1 components are arranged in series, while current traverses through the C_2 and R components. The input voltage is elevated and conveyed to the output [30], [31].

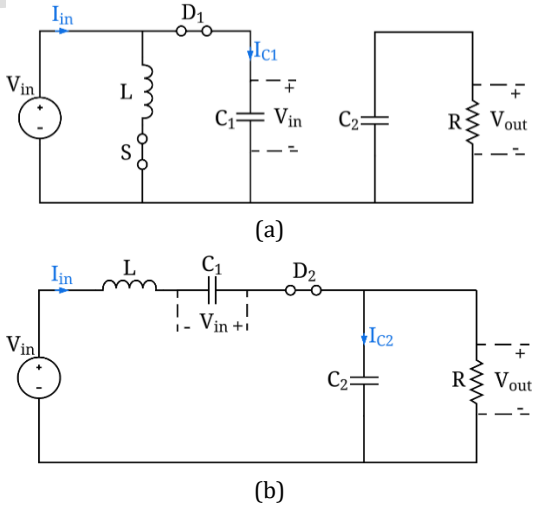

Figure 6. Super-lift Luo converter circuit. (a): switch on. (b): switch off.

The circuit equations for the open/closed switch scenario are delineated in Equations (9-12).

Switch on;

$$I_{in} = I_L + I_{C_1} \tag{9}$$

$$I_{in} = I_L + \left(\frac{1-k}{k}\right) \times I_L = \frac{I_L}{k} \tag{10}$$

$$I_{C_1} = \left(\frac{1-k}{k}\right) \times I_L \tag{11}$$

Switch off;

$$I_{in} = I_L = I_{C_1} \tag{12}$$

I_{in} represents the input current, I_L denotes the inductor current, and I_{C1} signifies the current traversing the C_1 capacitor.

Upon closing the switch, energy is accumulated in the C_1 capacitor as a result of the input. Upon opening the switch, the C_1 capacitor, positioned in series with the inductor element, acts as a source, supplying the load and the C_2 capacitor. The voltage across the C_1 capacitor at the instant the switch is closed and at the conclusion of the switch being opened is specified in Equations (13 and 14), respectively.

$$V_{C_1} = V_{in} - \Delta V_{C_1} = V_{in} - \frac{t}{C_1} I_L \tag{13}$$

$$\Delta V_{C_1} = \frac{1}{C_1} \int_{kT}^{T} I_L dt = \frac{1-k}{C_1} T I_L \tag{14}$$

When the switch is opened, the C_2 capacitor, which is charged, feeds the resistive load by forming a closed loop with the resistive load due to the D_2 diode being in the off state when the switch is closed. When the switch is in the open position and at the end of the closed position, the voltage across the C_2 capacitor is given in Equations (15 and 16), respectively.

$$V_{C_2} = V_{out} - \frac{t}{C_2} I_{out} = V_{out}\left(1 - \frac{t}{RC_2}\right) \tag{15}$$

$$\Delta V_{C_2} = \frac{k}{f_s \times R \times C_2} V_{out} \tag{16}$$

The voltage variations across these two capacitors in the circuit are analyzed, and the change in the output voltage is given by Equation (17).

$$\Delta V_0 = \Delta V_{C_1} + \Delta V_{C_2} = \left(\frac{1}{C_1} + \frac{k}{C_2}\right) \frac{V_0}{f_s \times R} \tag{17}$$

In this context, f_s denotes the switching frequency, while T represents the time. ΔV_{C_1} and ΔV_{C_2} represent the terminal voltages across the C_1 and C_2 capacitors, respectively [32], [33].

These circuit equations facilitate the representation of the waveforms for the output voltage, input current, and the current through the C_1 capacitor. The waveforms are depicted in Figure (7).

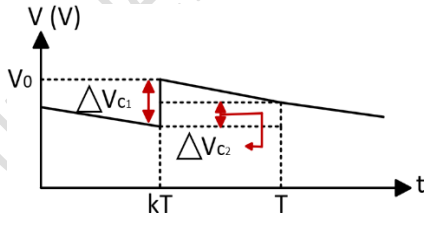

(a)

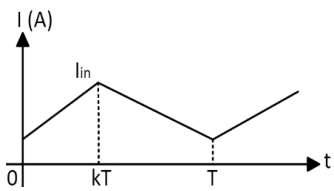

(b)

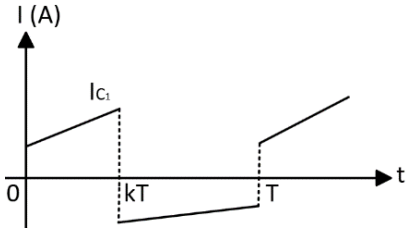

(c)

Figure 7. Waveforms. (a): output voltage. (b): input current. (c): current through the C_1 capacitor.

4 Fuzzy logic

Zadeh, the pioneer of fuzzy logic (FL), asserted that this approach mirrors human cognitive processes, making it appropriate for scenarios lacking clear determinations [34]. FL eliminates the necessity for a mathematical model and definitive input data in the regulation of nonlinear systems [35].

FL employs numerous membership functions, including triangular, trapezoidal, sigmoid, Gaussian, and bell curve [36], [37]. The triangular membership function, commonly used in solar energy systems, encompasses three states [38]. Consequently, in this function, the membership values are presented as specified in Equation (18).

$$\mu_A(x) = \mu_A(x: a, b, c) = \begin{cases} (x-a)/(b-a), a \le x \le b \\ (c-x)/(c-b), b \le x \le c \\ 0, x > c \ \vee x < a \end{cases} \tag{18}$$

In this context, a, b and c denote the values of the membership function, arranged in the sequence $a < b < c$.

4.1 The operational principle of fuzzy logic

The FL system comprises a knowledge base, fuzzification, inference, and defuzzification components. The knowledge base comprises data and rule bases. The rule base contains rules created using traditional If-Then-Else structures for system control. Figure (8) illustrates the process block diagram of the FL system.

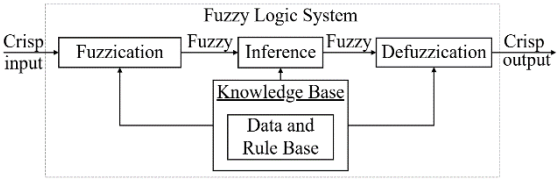

Figure 8. Block diagram of a FL system.

The fuzzification unit constitutes the initial component of the fuzzy system. This unit integrates input data with fuzzy sets through the application of membership functions. The established fuzzy values are conveyed to the inference unit utilizing the rules from the rule basis. The derived fuzzy outputs are transformed into crisp outputs within the defuzzification unit for application in the system [35], [39].

The error and rule bases established for FL are formulated in alignment with the system to be controlled. Consequently, they may also function as MPPT algorithms in photovoltaic systems. In contrast to alternative control methods, it autonomously establishes the input-output connection for the system requiring control. This facilitates controller design without requiring supplementary definitions.

MPPT algorithms utilizing FL typically employ two inputs: error and the rate of change of error. The maximum operating point is characterized as the juncture at which power remains constant relative to the operating voltage, with the error and its variation articulated by Equations (19 and 20), respectively.

$$E(k) = (P(k) - P(k-1))/(V(k) - V(k-1)) \quad (19)$$

$$\Delta E(k) = E(k) - E(k-1) \quad (20)$$

The current state is represented by k, whereas the preceding state is shown by k-1 [40].

5 System design and evaluation

The study examines the enhancement of a PV panel's output voltage -under similar specifications- using two distinct converter topologies: the conventional boost converter and the super-lift Luo converter, both regulated by a fuzzy logic control strategy. To achieve this, MATLAB/Simulink environment was chosen to design, construct, and assess the performance of these systems under diverse environmental conditions, owing to its block-based modeling framework, comprehensive component libraries, and robust capabilities in dynamic system analysis. Its suitability for power electronics and intelligent control applications facilitated accurate modeling of the converters and efficient simulation of their real-time performance. The entire simulation time was set to 1 second to accurately capture rapid transient responses to variations in irradiance and temperature, allowing for a precise comparison of dynamic performance. Figure (9) displays the comprehensive circuit schematics of the two designed systems.

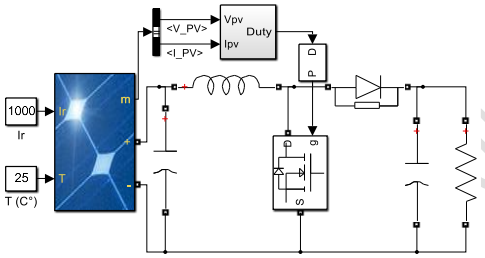

(a)

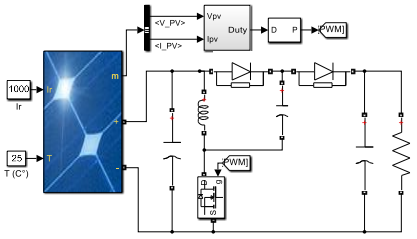

(b)

Figure 9. The engineered solar energy system. (a): employing a boost converter. (b): employing a super-lift Luo converter.

The PV panel values utilized in the study are not affiliated with any particular brand but were derived from the selection of appropriate values based on existing literature. Table 2 shows the chosen PV panel parameter values necessary for attaining optimal system efficiency. The PV panel values have remained consistent for systems engineered with conventional boost and super-lift Luo converters.

Table 2. PV panel features.

Parameters	Values
Parallel strings: n_p	5
Series-connected modules per string: n_s	5
Cells per module: N_{cell}	54
Maximum power: P_{mp} (W)	1575.7875
Voltage at maximum power point: V_{mp} (V)	33.35
Current at maximum power point: I_{mp} (A)	9.45
Open circuit voltage: V_{oc} (V)	40.85
Short-circuit current: I_{sc} (A)	9.98
Temperature coefficient of V_{oc} (%/°C)	-0.29
Temperature coefficient of I_{sc} (%/°C)	0.05

The internal structure of the FLC designed for the control of converters is shown in Figure (10). The current and voltage data acquired from the PV panel is compared with the preceding (k-1) state utilizing memory blocks. The error and its variation are computed in this manner. The error and the modification in the error data are assessed in the established rule table to produce the triggering signal. The signal derived from the FLC output is calibrated to a range of 0-1 via the PWM Generator block, converting it into a suitable triggering signal for the converter's switching element.

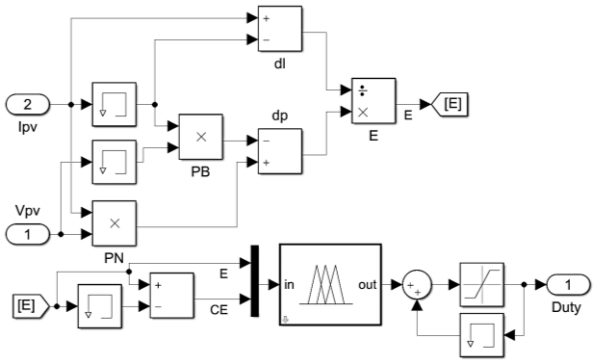

Figure 10. The internal structure of the developed FLC.

The fuzzy rules formulated for the regulation of classical boost and super-lift Luo converters utilized in the solar energy system are presented in Tables 3 and 4, respectively. In the study, five membership functions were established for the inputs of both converters, yielding a total of 25 rules. In the conventional boost converter, power and voltage parameters were utilized as inputs to minimize the error rate. The system has attained optimal performance.

Table 3. Rule table for the boost converter.

Vn/Pv	NB	NS	ZE	PS	PB
NB	ZE	ZE	PB	PB	PB
NS	ZE	ZE	PS	PS	PS
ZE	PS	ZE	ZE	ZE	NS
PS	NS	NS	NS	ZE	ZE
PB	NB	NB	NB	ZE	ZE

The input voltage value was utilized in the rule table formulated for the super-lift Luo, as presented in Table 4. The process is conducted by analyzing the error, its variation, and the rate of change of the error. In the rule base, the definitions with negative values (NS, NB) yield a voltage that is below the reference for the converter, resulting in a reduced estimated duty-cycle ratio. The FLC system facilitates the attainment of optimal power by endeavoring to enhance this ratio. Moreover, positive values correspond to an increased duty cycle, thereby

contributing to the regulation of the output voltage. The fuzzy rule base was constructed according to delta error values observed through voltage variation analysis, and the rule table was developed using a trial-and-error approach to fine-tune the system performance.

Table 4. Rule table for the super-lift Luo converter.

Error/ΔError	NB	NS	ZE	PS	PB
NB	NB	NB	NS	NS	ZE
NS	NB	NS	NS	ZE	PS
ZE	NS	NS	ZE	PS	PS
PS	NS	ZE	PS	PS	PB
PB	ZE	PS	PS	PB	PB

Membership functions delineate the fuzzy set distribution of input and output variables and are essential in establishing the rule base. In this study, triangular membership functions were selected due to their ability to provide sharper and more precise responses in converter control applications. The initial input membership function and the defined ranges of the two planned systems exhibit discrepancies. The voltage range of the Luo converter exceeds that of the classical boost converter, resulting in a broader definition range for the membership functions. Membership function parameters were determined based on the converters' operating voltage ranges to ensure accurate fuzzification of system variables. Figure (11) illustrates the membership functions developed for the traditional boost and super-lift Luo converters.

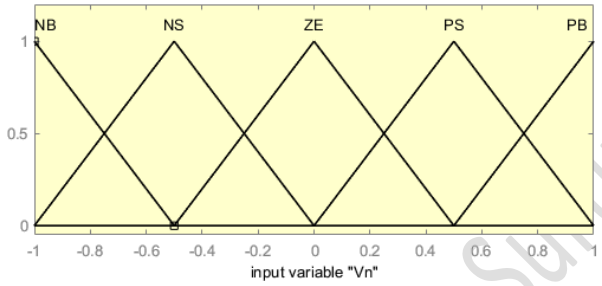

(a)

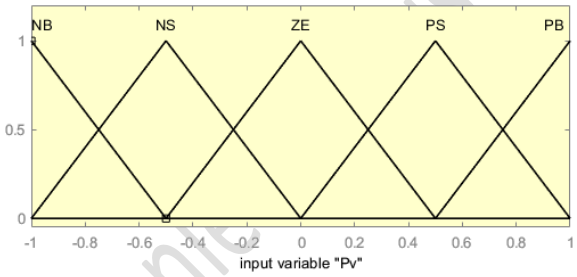

(b)

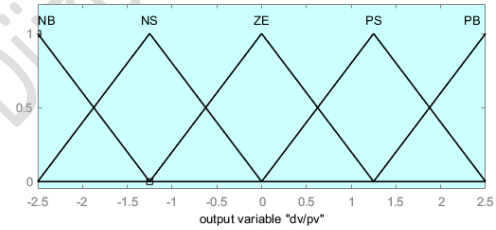

(c)

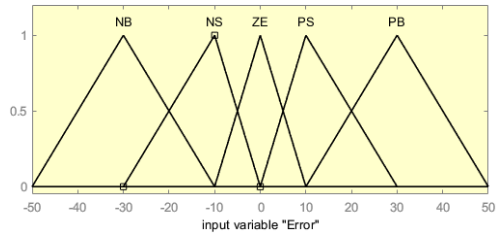

(d)

Figure 11. Membership functions for boost and super-lift Luo converters. (a): first input of boost. (b): second input of boost. (c): output of boost. (d): first input of super-lift Luo.

Figure (12) illustrates the control surface derived from the FLC structure designed for super-lift Luo. The rapid switching of the Luo converter results in several harmonics in the surface graph. The yellow zone on this surface, delineated by the error and error variation specified in Equations (4 and 5), represents the system's optimal operating region.

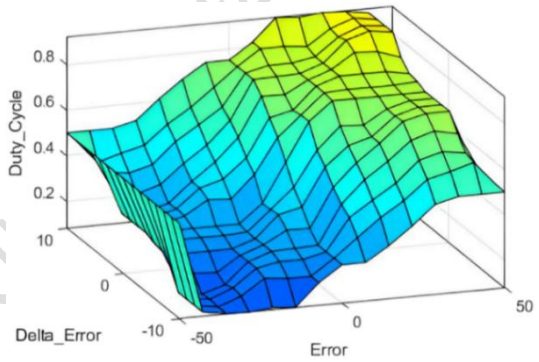

Figure 12. The FLC control surface of the super-lift Luo converter.

A parallel capacitor (C_{PV}) is situated between the solar panel and the converter. The primary purpose of this improvement is to deliver a more constant input voltage to the converter by filtering the fluctuating voltage from the PV panel. The circuit specifications of the parallel-connected capacitor and the converters utilized are presented in Table 5. The switching frequencies of the boost and super-lift Luo converters have been selected differently due to structural differences; however, the input currents have been kept approximately equal. This approach facilitates the examination of the voltage values that the converters can provide under similar operating conditions, thereby ensuring a fair comparison in performance evaluations.

Table 5. The circuit parameters of the converters.

Components	Boost Converter	Super-lift Luo Converter
Parallel Capacitor (C_{PV})	833 µF	4400 µF
Switching Frequency	5 kHz	76 kHz
Inductor (L)	0.1 mH	5 mH
Capacitor (C_1)	4266 µF	1100 µF
Capacitor (C_2)	-	1100 µF
Resistor (R)	7.5 Ohm	80 Ohm

The input voltage and input current graphs derived from the PV panel, utilizing the circuit parameters specified in Table 5, are illustrated in Figure (13). In the circuit utilizing the super-lift Luo, it has been seen that the input current is significantly lower than that of the traditional boost converter circuit. This

scenario originates from the circuit schematic of the Luo converter. The converter facilitates the attainment of high voltage at low currents.

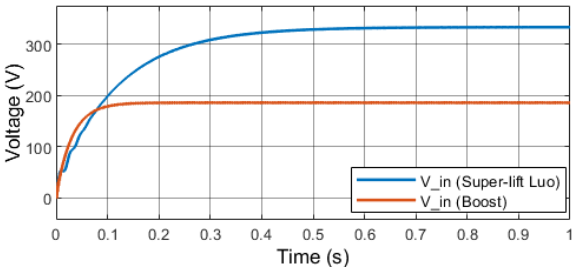

(a)

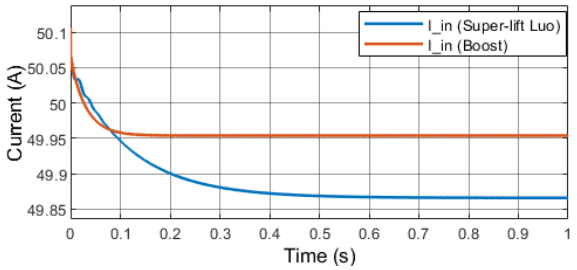

(b)

Figure 13. Input graphics. (a): voltage. (b): current.

The values derived from the PV panel include the current, voltage, and power graphs received from the converter outputs, as illustrated in Figure (14). The graphs demonstrate that significantly greater voltages are achieved using the super-lift Luo converter in comparison to the traditional boost converter. Moreover, although the Luo converter achieves a reduced current, its output power surpasses that of the conventional boost converter. The system utilizing the super-lift Luo rapidly mitigates initial oscillations, thus preventing generation of harmonics. Nevertheless, the system designed with the conventional boost converter attains a stable state more rapidly. Furthermore, both systems can generate a consistent voltage level without overshooting.

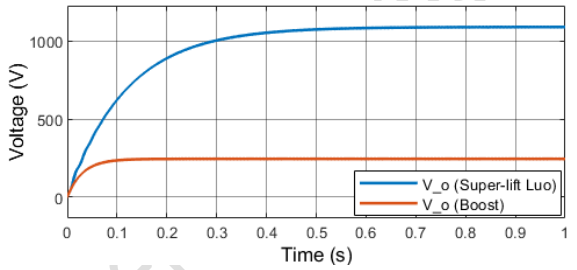

(a)

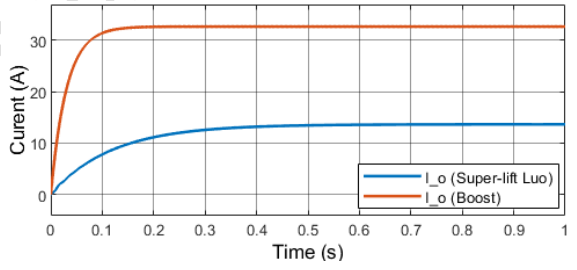

(b)

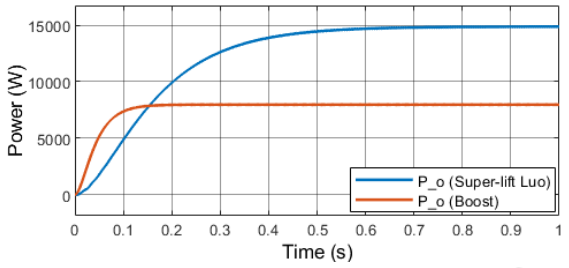

(c)

Figure 14. Output graphics. (a): voltage. (b): current. (c): power.

The ultimate state values derived from the engineered circuits are displayed in Table 6. This data indicates that the super-lift Luo converter enhances both the power output from the PV panel and delivers superior voltage and efficiency levels.

Table 6. The final values and settlement durations obtained from the systems.

Parameters	Boost Converter	Super-lift Luo Converter
Input Voltage (V)	186.6	335.2
Input Current (A)	49.95	49.86
Input Power (W)	9305	16650
Output Voltage (V)	245.8	1091
Settling Time (s)	0.12	0.5
Output Current (A)	32.78	13.64
Output Power (W)	7981	14870
Efficiency (%)	85.77	89.34

To examine the dynamic response of the systems under fluctuating environmental conditions, the temperature and irradiance values applied to the PV panel were modified as illustrated in Figure (15). The temperature was reduced linearly from 25 °C to 15 °C over 0.25 s, held constant until 0.45 s, and then increased linearly to 28 °C by 0.75 s, where it stabilized for the remainder of the experiment. The irradiance level initially started at 1000 W/m^2 and decreased linearly to 850 W/m^2 within 0.2 seconds. It remained constant until 0.4 s, followed by a linear increase to 1050 W/m^2 by 0.75 s, following which it remained stable until the end of the 1-second simulation.

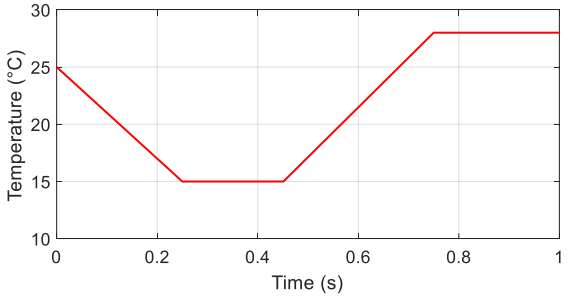

(a)

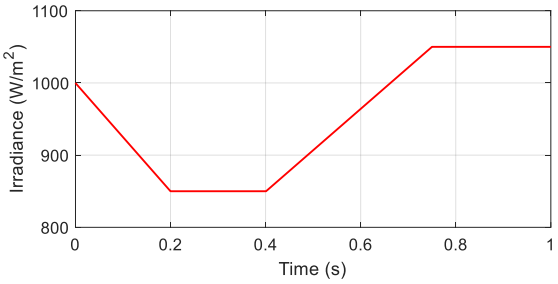

(b)

Figure 15. Graphs of the variable parameters applied to the PV panel. (a): temperature. (b): irradiation.

Figure (16) illustrates the output current, voltage, and power characteristics of both converters under different irradiance and temperature conditions. Under these conditions, it was noted that the current component significantly influenced the output power of PV panel; owing to the current's direct reaction to variations in irradiance and temperature, the power graph displayed more pronounced fluctuations than the voltage graph. Among the two topologies, the super-lift Luo converter exhibited less sensitivity to fluctuations in irradiance and temperature, displaying more seamless power changes. The FLC used in MPPT algorithm proficiently regulated the system's transient behavior, ensuring both converters reacted rapidly and reliably to changing conditions. It was noted that following the transient process, the output values aligned with the reference values established under constant conditions. The results demonstrate that FLC, by its adaptive control functionality, mitigates power fluctuations, thus improving the continuity and stability of system.

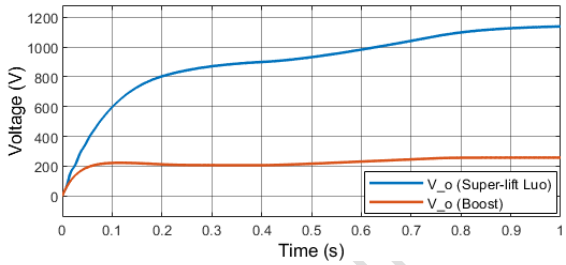

(a)

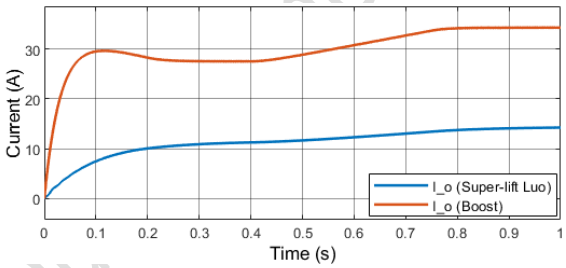

(b)

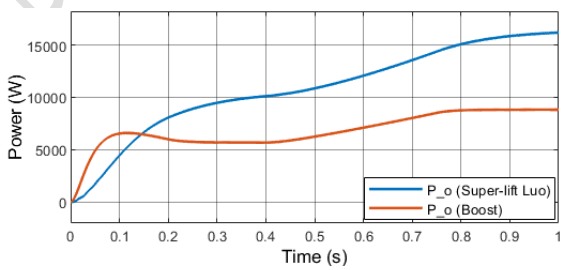

(c)

Figure 16. Output graphs with variable irradiation and temperature. (a): voltage. (b): current. (c): power.

To ensure the converters functioned under identical load settings, the boost converter circuit characteristics were modified in the study. The revised specifications for the boost converter circuit are detailed in Table 7.

Table 7. Revised parameters for the boost converter.

Components	Boost Converter
Parallel Capacitor (C_{PV})	1600 µF
Inductor (L)	0.5 mH
Capacitor (C)	6000 µF
Resistor (R)	80 Ohm

The two converters were evaluated under identical load conditions, and the resultant output current-voltage statistics are illustrated in Figure (17). The load resistance was adjusted to 75, 80, and 85 Ω, and the system responses were assessed. Both converters attained a stable voltage under varying loads; notably, the early transient oscillations in the super-lift Luo converter diminished with increasing load. Conversely, the output current in the boost converter demonstrated greater ripple, and the current magnitude diminished as the parameter values increased. This condition has adversely affected the system efficiency due to increased energy transmission losses. For instance, with an 80 Ω load, the super-lift Luo converter has an efficiency of 89.34%, whilst the boost converter maintains an efficiency of 75.96%. These findings demonstrate that the super-lift Luo converter has enhanced stability in transient behavior during load variations and offers superior overall system efficiency.

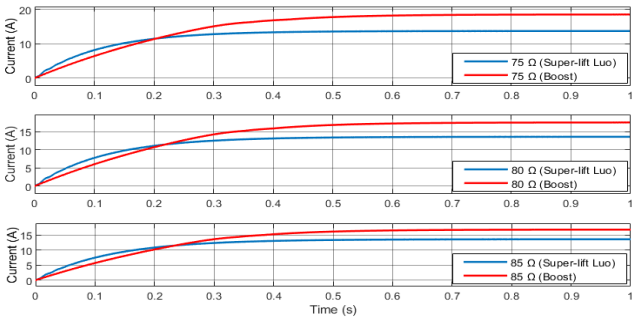

(a)

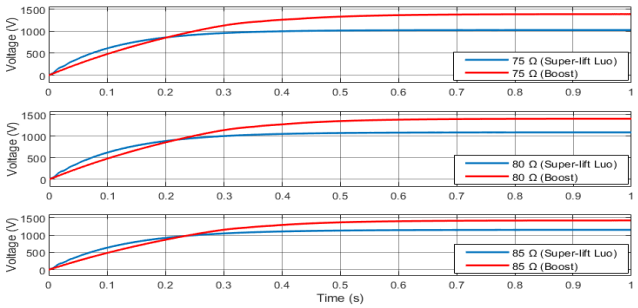

(b)

Figure 17. Output graphs for varying load conditions. (a): current. (b): voltage.

6 Conclusion

Two systems employing the same PV panel types and different converter types were assessed using FLC. The standard boost converter system achieved a low voltage output of 245.8 V and a high current of 32.78 A, rendering it suitable for residential loads. The system employing the super-lift Luo converter achieved an output voltage of 1091 V and a current of 13.64 A. This output, however excessive for a residential system, can be utilized across several sectors, including specialized DC loads operating at high voltage, HVDC distribution, industrial applications, data centers, electric vehicle charging stations, and large-scale battery systems.

Concerning settling durations, the conventional boost converter demonstrates greater speed; however, the increased power output of the super-lift Luo converter explains this difference. Besides, neither system demonstrates overshoot, and both achieve stable output levels.

In simulation performed under fluctuating environmental conditions (irradiation and temperature), both converters effectively managed transient behavior due to the FLC-based MPPT control framework and rapidly attained reference values. The super-lift Luo converter has exhibited enhanced transient performance, characterized by reduced voltage ripple and a more stable voltage level throughout fluctuating load situations. Furthermore, it has been noted that the level of oscillation in this converter diminishes as the load resistance increases. Conversely, substantial variations were seen in the output current of the boost converter as the load increased, but the efficiency stabilized around 75.96%. Conversely, the super-lift Luo converter exhibited a more stable and efficient solution, with an efficiency of approximately 89.34%. The findings demonstrate that the employed converter topology directly influences both output magnitudes of variables and the system's reaction to environmental and load-related variables. Consequently, choosing the suitable converter type for the application domain is essential for the system's overall performance and this study clearly demonstrates how the choice of DC-DC converter topology affects system efficiency.

For future work, it is recommended to apply advanced optimization techniques such as Genetic Algorithms, Particle Swarm Optimization, or other metaheuristic methods to tune the fuzzy membership functions, rule base, and scaling parameters to further enhance the FLC performance. Additionally, a comparison with Type-2 fuzzy controllers or the adoption of novel modeling techniques could be conducted to provide deeper insights and improve the control robustness and dynamic response of the system.

7 Author contribution statements

In this study, Author 1 contributed to the supervision and article administration. Author 2 contributed to the methodology, writing–original draft preparation, and resources. Author 3 contributed to the resources. Author 1, Author 2, and Author 3 contributed to the writing, reviewing, and editing of the article. All authors participated in the development of the idea.

8 Ethics committee approval and conflict of interest statement

"There is no need to obtain an ethics committee approval for the article prepared".

"There is no conflict of interest with any person / institution in the article prepared".

9 References

[1]Koca YB. "Fuzzy logic-based simulation and modelling of grid integration renewable energy systems for sustainable energy". *Niğde Ömer Halisdemir Üniversitesi Mühendislik Bilimleri Dergisi*, 14(1), 80–89, 2025.

[2]Mustafa AF. ''Bulanık Mantık Denetleyici Kullanılarak MPPT Performansının İyileştirilmesi''. *Kocaeli University, Master Thesis*, 2023.

[3]Nzoundja Fapi CB, Tchakounte H, Hamida MA, Wira P, and Kamta M. ''Experimental Implementation of Improved P&O MPPT Algorithm based on Fuzzy Logic for Solar Photovoltaic Applications''. *11th International Conference on Smart Grid, icSmartGrid 2023*, Paris, France, June 2023.

[4]Eshete FA, Samajdar DP, and Kumar A. ''Analysis of FLC Technique with P&O Algorithm under Variable Weather Condition''. *2023 IEEE Devices for Integrated Circuit (DevIC), IEEE*, Kalyani, India, April 2023.

[5]Lüy M, Metin NA, and Civelek Z. ''Maximum Power Point Tracking with Incremental Conductance and Fuzzy Logic Controller in Solar Energy Systems''. *El-Cezeri Journal of Science and Engineering*, 11(1), 120–130, 2024.

[6]Derbeli M, Napole C, and Barambones OA. ''Fuzzy Logic Control for Maximum Power Point Tracking Algorithm Validated in a Commercial PV System''. *Energies,* 16(2), 1-14, 2023.

[7]Çakmak F, Aydoğmuş Z, and Tür MR. ''Analyses of PO-Based Fuzzy Logic-Controlled MPPT and Incremental Conductance MPPT Algorithms in PV Systems''. *Energies*, 18(2), 1-22,2025.

[8]Larabı Z. ''Comparatıve study of dıfferent mppt algorıthms on 250kw grıd-connected pv system''. *İstanbul Aydın University, Master Thesis*, 2023.

[9]Wakchaure SD, and Mittal SK. ''Fuzzy Logic MPPT Techniques in Solar Photovoltaic System''. *International Journal for Research in Applied Science and Engineering Technology*, 9(9), 603–605, 2021.

[10]Teke M, Al-Arjeelı ASM, and Korkmaz F. ''Design and Comparison of MPPT Controller for PV Systems''. *International Journal of Engineering Research and Development*, 15(1), 1–15, 2023.

[11]Shukla A, & Mohaney SA. ''Complete review of FLC MPPT Technique and Comparison with INC Technique''. *International Journal for Research in Applied Science and Engineering Technology (IJRASET)*, 10(6), 1245–1253, 2022.

[12]Chandini G, Nikhila K, Hanumanth Reddy E, Kazol D, Amruth Kumar A, & Narasimhulu N. ''Performance Comparison of FLC MPPT with P & O and Incremental Conductance MPPT For standalone PV System''. *International Journal for Research in Applied Science and Engineering Technology (IJRASET)*, 10(6), 2879–2885, 2022.

[13]Yap KY, Sarimuthu CR, and Lim JM. ''Artificial intelligence based MPPT techniques for solar power system: A review''. *Journal of Modern Power Systems and Clean Energy,* 8(6), 1043-1059, 2020.

[14]Chamundeeswari V, and Niraimathi R. ''An efficient hybrid approach for high-gain DC–DC converter for hydropower

operated plants on DC load with super-lift converters''. *Electrical Engineering*, 107(1), 1315–1329, 2025.

[15]Ganga Bhavani CS, Bhanu Prasad N, and Ravi Kishore D. ''Enhancing Grid-Connected Hybrid Renewable Energy System with Super Lift Luo Converter for Improved Power Management and Reduced THD''. *Journal of The Institution of Engineers (India): Series B*, 106(1), 129–143, 2025.

[16]Karthikeyan K, Jayanthi S, and Gokulakrishnan R. ''High gain super lift Luo converter for hybrid energy management systems''. *International Journal of Science and Research Archive*, 13, 1318–1331, 2024.

[17]Chitra L, and Kumari KS. ''Power Quality Enhancements of AC Grid Using Luo Converter with GWO Based MPPT''. *2023 IEEE 8th International Conference for Convergence in Technology (I2CT)*, IEEE, Lonavla, India, April 2023.

[18]Kocalmış Bilhan A, and Emikönel S. "Design of P&O and FL based MPPT controllers of PV array by using positive super lift DC/DC boost converter". *International Journal of Energy and Smart Grid (IJESG)*, 7(1-2), 36–46, 2022, doi: 10.55088/ijesg.1201016.

[19]Gani A. ''Advanced controller design based on interval type-2 fuzzy neural network for elementary super-lift Luo converter''. *Transactions of the Institute of Measurement and Control*, 47(10), 1953-1963, 2024.

[20]Keçecioğlu O. F. ''Design of type-2 fuzzy logic controller optimized with firefly algorithm for maximum power point tracking of photovoltaic system based on super lift Luo converter''. *International Journal of Numerical Modelling: Electronic Networks, Devices and Fields,* 35(4), 1-17, 2022.

[21]Prem KS, Ezhileesha V, Sharmitha D, and Arun RR. ''An improved P&O based optimization control algorithm for voltage improvement in stand-alone PV system''. *2023 2nd International Conference on Advancements in Electrical, Electronics, Communication, Computing and Automation (ICAECA)*, IEEE, Coimbatore, India, June 2023.

[22]Mohammad KA, and Musa SM. ''Enhancement of solar energy utilization through an artificial neural network controller featuring a dynamic learning rate and a positiveoutput super lift luo converter''. *World Journal of Advanced Engineering Technology and Sciences*, 12(2), 663–673, 2024.

[23]Kevat V, Sakhare A, and Mikkili S. ''Design of Non-isolated DC–DC Converters for Maximum Power Point Tracking in Stand-Alone Photovoltaic System''. *Transactions of the Indian National Academy of Engineering*, 1–31, 2025.

[24]Salım RYA. ''Güneş enerjisi sisteminin performansını iyileştirmek için bulanık mantığa dayalı maksimum güç noktası takip algoritması''. *Kastamonu University, Master Thesis*, 2021.

[25]Shaikh AM, Shaikh MF, Shaikh SA, Krichen M, Rahimoon RA, and Qadir A. ''Comparative analysis of different MPPT techniques using boost converter for photovoltaic systems under dynamic shading conditions''. *Sustainable Energy Technologies and Assessments*, 57(2023), 103259, 2023.

[26]Kumar AM, and Karuvelam PS. ''PV Fed EV Charging System Based on Re-lift Luo Converter and DAB Converter''. *Journal of Electrical Engineering & Technology*, 18(4), 2609–2621. 2023.

[27]Wang M, Gao B, Lei J, Quan X, and Guan Y. ''Improved White Shark Optimizer Based Maximum Power Point Tracking Algorithm for Photovoltaic Systems Under Partial Shading Conditions''. *Journal of Electrical Engineering & Technology*, 20(3), 1293–1306, 2025.

[28]Kaba B, Şahin ME, and Tören M. ''Yükselten Tip DA/DA Dönüştürücü Kontrolünün Farklı Kontrol Yöntemleriyle Batarya Kaynağı için İncelenmesi''. *EMO Bilimsel Dergi*, 15(1), 15–26, 2025.

[29]Jin GG, Mengesha KA, and Son YD. ''Integral Sliding Mode Control of a DC-DC Boost Converter with Uncertainties''. *Journal of Electrical Engineering & Technology*, (0123456789), 2025.

[30]Luo FL, and Ye H. ''Positive output super-lift converters''. *IEEE Transactions on Power Electronics*, 18(1), 105–113, 2003.

[31]El-Ghanam SM. ''Design, implementation and performance analysis of positive super-lift Luo-converter based on different MOSFET types''. *Indian Journal of Physics*, 94(6), 833–839, 2020.

[32]Luo FL, and Ye H. *Advanced DC/DC Converters*. 2nd ed. Boca Raton, Florida, ABD: CRC Press, 2016.

[33]Luo FL. ''Analysis of super-lift Luo converters with capacitor voltage drop''. *2008 3rd IEEE Conference on Industrial Electronics and Applications, ICIEA 2008*, Singapur, July 2008.

[34]Zadeh LA. ''Fuzzy sets''. *Information and Control*, 8(3), 338–353, 1965.

[35]Nasser KW, Yaqoob SJ, and Hassoun ZA. ''Improved dynamic performance of photovoltaic panel using fuzzy logic-MPPT algorithm''. *Indonesian Journal of Electrical Engineering and Computer Science*, 21(2), 617–624, 2020.

[36]Emikönel S. ''Güneş enerji tesisleri için bulanık mantık kontrollü maksimum güç noktası takip algoritmasının geliştirilmesi ve incelenmesi''. *Nevşehir Hacı Bektaşi Veli University, Master Thesis*, 2022.

[37]Samavat T, Nazari M, Ghalehnoie M, Nasab MA, Zand M, Sanjeevikumar P, and Khan BA. ''Comparative Analysis of the Mamdani and Sugeno Fuzzy Inference Systems for MPPT of an Islanded PV System''. *International Journal of Energy Researc*, 2023(1), 7676113, 2023.

[38]Vinitha JC, Ramadas G, and. Rani PU. ''PSO Based Fuzzy Logic Controller for Load Frequency Control in EV Charging Station''. *Journal of Electrical Engineering & Technology*, 19(1), 193–208, 2024.

[39]Ross TJ. *Fuzzy Logic With Engineering Applications*. 3rd ed. Chichester, UK: WILEY, 2010.

[40]Menzri F, Boutabba T, Benlaloui I, Bawayan H, Mosaad MI, and Mahmoud MM. ''Applications of hybrid SMC and FLC for augmentation of MPPT method in a wind-PV-battery configuration''. *Wind Engineering*, 48(6), 1186–1202, 2024.